The Anisotropic Transfer of Resonance Photons in Hot Plasmas on Magnetized White Dwarfs

Yukikatsu TERADA,[1] Manabu ISHIDA,[2] and Kazuo MAKISHIMA[1,3]

[1]*Cosmic Radiation Laboratory, RIKEN, 2-1 Hirosawa, Wako, Saitama 351-0198*
[2]*Department of Physics, Tokyo Metropolitan University, 1-1 Minami-Ohsawa, Hachioji, Tokyo 192-0397*
[3]*Department of Physics, School of Science, The University of Tokyo, 7-3-1 Hongo, Bunkyo-ku, Tokyo 113-0033*
terada@riken.jp

Abstract

In order to confirm the anisotropic effect of resonance photons in hot accretion columns on white dwarfs in magnetic cataclysmic variables, proposed by Terada et al. (2001), systematic studies with ASCA of 7 polars and 12 intermediate polars were performed. The equivalent widths of He-like Fe Kα lines of polars were found to be systematically modulated at their spin periods in such a way that it increases at the pole-on phase. This implies that the anisotropic mechanism is commonly operating among polars. On the other hand, those of intermediate polars are statistically consistent with being unmodulated with an upper limit of 1.5-times modulation. This may be due to a different accretion manner, like an aurora curtain (Rosen et al. 1988), so that the plasma also becomes optically thin along the horizontal axis for the resonance lines, or because of larger optical depths for Compton scattering if the emission regions have the same coin-like shapes as polars.

1. Introduction

A magnetic cataclysmic variable (MCV) is a close binary consisting of a white dwarf (WD) and a mass-donating companion star. Matter that spills over the Roche lobe of the companion star accretes on a magnetic pole of the WD, forming a post-shock hot plasma (Patterson 1994 and references therein). According to a systematic X-ray study of MCVs by Ginga, their X-ray spectra can be described by optically thin thermal bremsstrahlung continua with Fe lines (Ishida 1991). These X-ray characteristics are approximately the same for both subgroups of MCVs, polars and intermediate polars (IPs). Plasma diagnostics with atomic lines, performed with ASCA (Fujimoto, Ishida 1997; Ezuka, Ishida 1999), confirmed the multi-temperature structure of the plasma as had been predicted by Hoshi (1973) and Aizu (1973).

Considering the typical size ($\sim 10^7$ cm) and density ($\sim 10^{15-16}$ cm^{-3}) of an accretion column of an MCV, the plasma is not completely optically thin; it is estimated to be marginally optically thick for Compton (or Thomson) scattering with an optical depth of order 0.1. Under such conditions, the atomic line structure is expected to be suppressed by 10%–20%, because the line photons would experience large shifts, reaching ~ 1 keV as they Compton scatter off hot electrons. At the same time, the plasma is optically thick for resonant photons of atomic lines from abundant heavy elements, including Fe in particular (Fujimoto, Ishida 1997). Then, the line structure of the resonance transitions would be more suppressed, because the resonant photons would be effectively trapped in the column, and escape most easily when they Compton scatter out of the resonance. Nevertheless, we usually observe many ionized atomic lines in the X-ray spectra of MCVs (Ezuka, Ishida 1999), and the apparent metal

abundances derived from the equivalent width (EW) of these lines are not much lower than one-times solar. In addition, some MCVs, called Pole-on line emitters (POLES; Terada et al. 2001, hereafter Paper I), including AX J2315−0592 (Misaki et al. 1996), RX J1802.1+1804 (Ishida et al. 1998), and AX J1842.8−0423 (Terada et al. 1999), exhibit extremely strong He-like Fe-K lines, having an EW of ~ 4000 eV, implying apparent Fe abundances of $\sim$ three-times solar.

In order to solve the puzzle of extremely strong Fe lines, we have developed a scenario of Fe-K line collimation along the vertical axis of the accretion column incorporating resonance scattering (Terada et al. 1999; Paper I; Terada 2002). The anisotropy occurs when the accretion column has a flat shape, and is augmented by the strong longitudinal velocity gradient in the accretion flow, which invalidates the resonance condition for line photons when they propagate along the vertical axis. Since the Fe ions are heavy, their thermal resonance width (typically ~ 3 eV for a 10 keV plasma) is easily exceeded by the vertical Doppler shift (~ 10 eV from the bottom to the top of the column). Therefore, the resonant trapping of Fe-K photons is preferentially reduced along the vertical axis, and hence the resonance line photons are collimated along the vertical direction. This scenario can explain both the lack of line destruction and the enigmatic POLE phenomenon.

We have numerically confirmed the anisotropic propagation of resonance photons via extensive Monte Carlo simulations (Paper I), employing the analytic solution to the post-shock flow by Aizu (1973), and the Fe line emissivities in hot plasma by Mewe, Gronenschild, and van den Oord (1985). The results show that the directional emissivity of the resonant Fe-K line photons is indeed enhanced by up to a factor of ~ 2–2.5. In addition, we have confirmed, through ASCA observations of the polar V834 Centauri, that the EW of its He-like Fe Kα line

Table 1. Objects analyzed in the present paper.

Object name		Date of observation (UT)	Exp. (ksec)* SIS	GIS	Cnt rate SIS	GIS	Phase 0.0 (HJD) in figures 1 and 2	Spin period (days)	Ref.[†]
Polars									
V834 Cen	(1)	1994/03/03.64–04.13	21.7	23.2	0.26	0.18	2445048.9500	0.070498	1
	(2)	1999/02/09.93–11.72	62.3	53.5	0.25	0.19			
AM Her	(1)	1993/09/27.22–28.27	30.9	43.5	0.61	0.43	2443014.76614	0.128927	2
	(2)	1995/03/06.84–07.22	18.3	16.8	0.92	0.66			
	(3)	1995/03/09.03–10.03	45.5	41.1	0.89	0.65			
BL Hyi		1994/10/11.47–12.59	41.4	43.5	0.21	0.16	2450379.4725	0.078915	3
BY Cam		1994/03/11.49–12.16	29.5	34.7	0.98	0.68	2446138.8202	0.13979	4
EF Eri		1993/07/23.90–24.77	35.9	39.0	0.93	0.61	2443894.6824	0.056266	5
RX J1015+0904		1999/05/04.08–05.41	54.0	54.0	0.09	0.07	2451302.500	0.055471	6
V2301 Oph		1998/09/28.49–30.21	70.6	73.0	0.21	0.15	2448071.02014	0.078450	7
Intermediate Polars									
AO Psc		1994/06/22.29–24.56	81.0	84.3	0.57	0.48	2444883.92074	0.00931948	8
BG CMi	(1)	1996/04/14.76–15.97	42.0	43.4	0.16	0.17	2450186.5	0.0105729	9
	(2)	1996/04/17.44–18.53	40.9	41.5	0.15	0.16			
EX Hya		1993/07/16.45–17.64	36.0	38.8	2.79	1.50	2437699.8914	0.0465465	10
FO Aqr		1993/05/20.93–02.04	37.8	38.0	0.27	0.32	2446097.243668	0.01451911	11
PQ Gem	(1)	1994/11/04.91–07.10	76.2	80.2	0.37	0.30	2449297.9730	0.009645994	12
	(2)	1999/10/19.71–20.31	35.0	42.9	0.37	0.28			
RX J1712−2414		1996/03/18.85–21.24	81.4	84.2	0.79	0.65	2450159.5	0.010737	13
TV Col		1995/02/28.25–01.44	36.7	39.9	0.65	0.54	2447139.524	0.02211	14
TX Col		1994/10/03.29–04.42	39.9	45.1	0.22	0.16	2449627.5	0.02212	6
V1062 Tau		1998/02/16.89–18.48	57.5	14.7	0.23	0.24	2450859.5	0.04313	9
V1223 Sgr		1994/04/24.18–25.96	57.0	59.2	1.23	1.00	2445626.13067	0.00862854	17
V405 Aur	(1)	1996/10/05.56–07.47	47.5	41.1	0.34	0.23	2449689.573466	0.006313154	15
	(2)	1999/03/21.40–22.44	39.0	43.3	0.38	0.26			
XY Ari	(1)	1995/08/07.00–07.91	34.6	34.9	0.14	0.15	2449935.5	0.00238773	16
	(2)	1996/01/28.21–29.73	58.5	61.0	0.16	0.16			
	(3)	1996/02/18.97–19.56	24.4	25.6	0.13	0.14			

* Averaged exposure of the two SIS detectors (SIS0 and SIS1) and that for the two GIS detectors (GIS2 and GIS3).

[†] References; 1: Schwope et al. (1993), 2: Heise and Verbunt (1988), 3: Mernickent, Diaz, and Arenas (1999), 4: Piirola et al. (1994), 5: Cropper (1985), 6: Norton et al. (1997), 7: Barwig, Ritter, and Barnbantner (1994), 8: Kaluzny and Semeniuk (1988), 9: Patterson (1994), 10: Bond and Freeth (1988), 11: Shafter and Macry (1987), 12: Hellier (1997), 13: Buckley et al. (1997), 14: Augusteijn et al. (1994), 15: Skillman (1996), 16: Takano et al. (1989), 17: ASCA Timing Analysis.

increases during pole-on phases of its rotation (Paper I). The proposed mechanism has thus been confirmed through calculations, and the observation of a few particular polars.

According to our Monte Carlo simulations, the anisotropic propagation of resonance Fe line photons should occur for a rather wide range of plasma parameters in the accretion column (Paper I). We hence expect to observe the rotational modulation of the resonant Fe-K line EW, not only in the particular case of V834 Centauri, but also of MCVs in general. In order to examine this conjecture, here we systematically analyze the ASCA data of 7 polars and 12 IPs.

2. Observation

The central aim of this paper is to describe our search of data for a possible dependence of the Fe line EW on the angle, θ, between our line-of-sight and the axis of the accretion column. We needed to perform spin-phase-resolved spectroscopy of the target MCVs. Accordingly, we analyzed all 9 polars and 13

IPs observed with ASCA satellite (Tanaka et al. 1994). Some objects (V834 Cen, EK UMa, and RX J1015+0904) are the approved targets of our proposal for this purpose, and the others are archived or published observations. After discarding objects that were too X-ray faint (< 0.05 GIS cnt s^{-1}) and those with insufficient exposure (< 20 ksec), we were left with 7 polars and 12 IPs, as listed in table 1, including V834 Centauri, the results for which are reported in Paper I. Their geometries, i.e., the inclination angle, i, and the pole colatitude, β, were obtained by polarimetric observations in the optical-to-ultraviolet band, and are summarized in table 4 of Paper I.

For each target, we accumulated the GIS (Ohashi et al. 1996; Makishima et al. 1996) and SIS (Burke et al. 1991) events within a circle of radius $4'.5$ centered on the object, employing the following data-selection criteria. We discarded the data during ASCA passage through the South Atlantic Anomaly, and when the field of view of ASCA was within $5°$ of the Earth's rim. Furthermore, we discarded the GIS data during
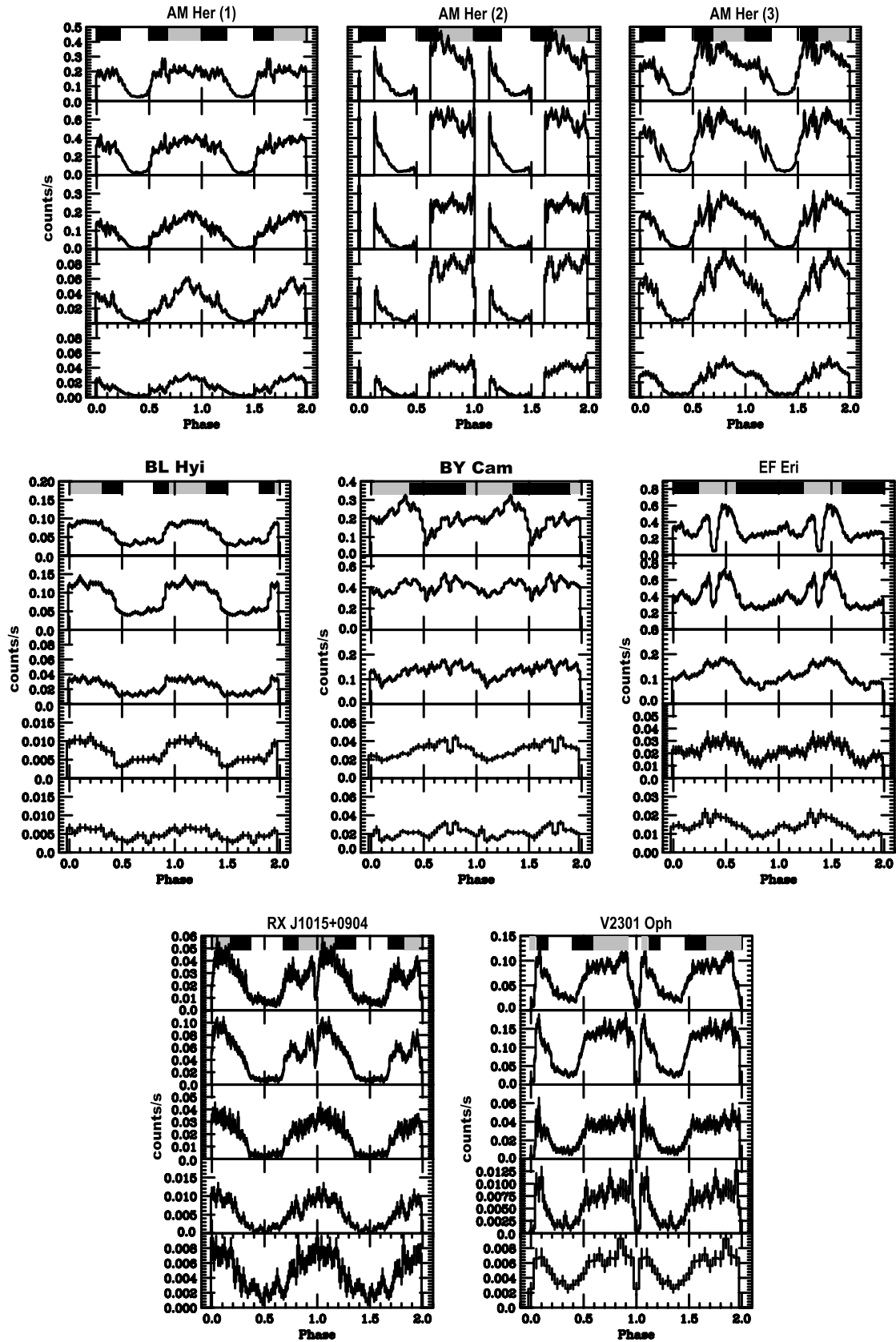
Fig. 1. X-ray light curves of the polars observed with ASCA, folded on their spin periods listed in table 1. The respective phase 0.0 is given in table 1. For each object, light curves in five energy bands (0.5–1.5, 1.5–4.0, 4.0–6.2, 6.2–7.2, and 7.2–10.0 keV from top to bottom) are presented. The pole-on and side-on phases are shown at the top of each panel by the gray and black bands, respectively (see the text). The data of V834 Cen is reported in Paper I.
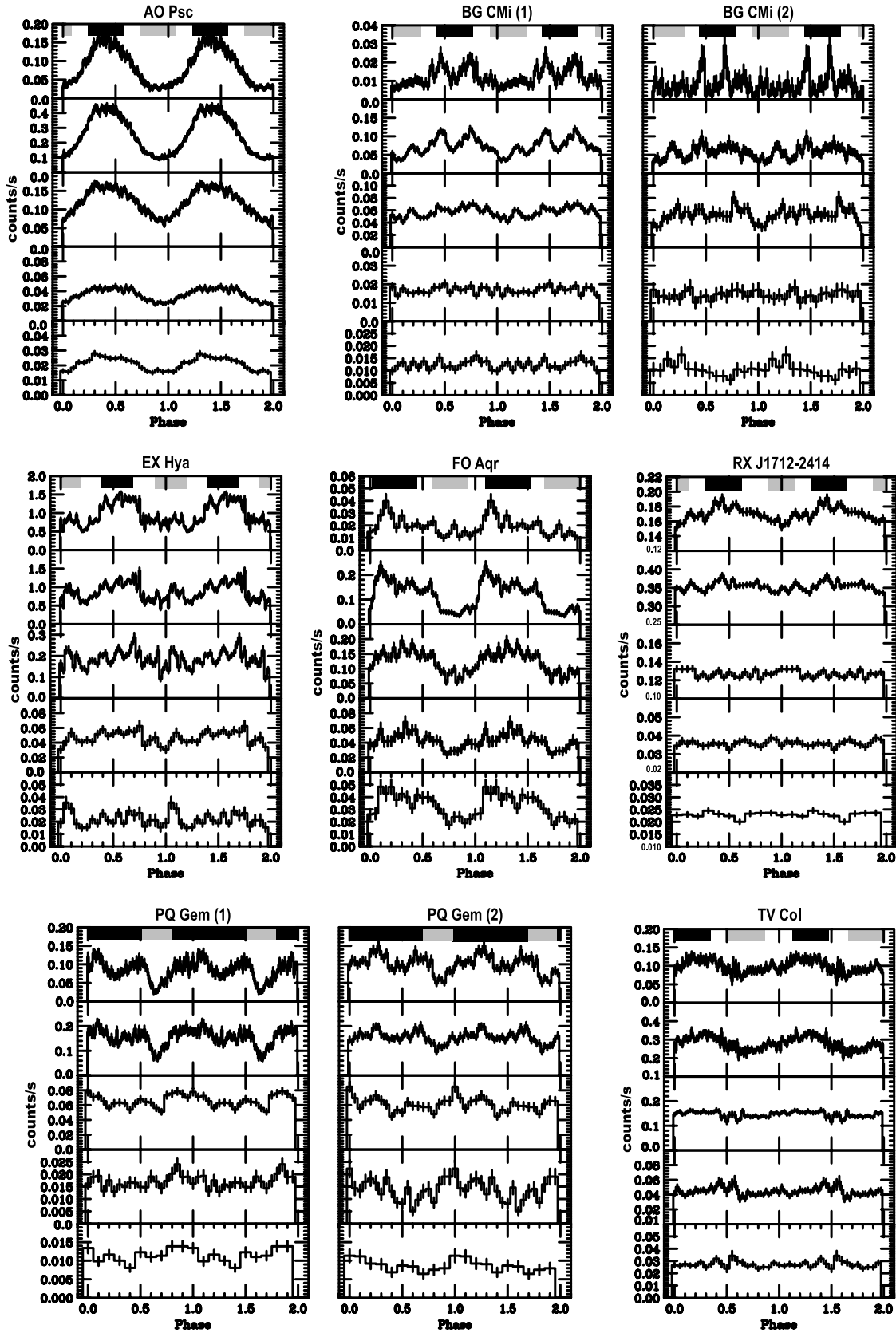
Fig. 2. Similar to figure 1, but for the IPs in our sample.
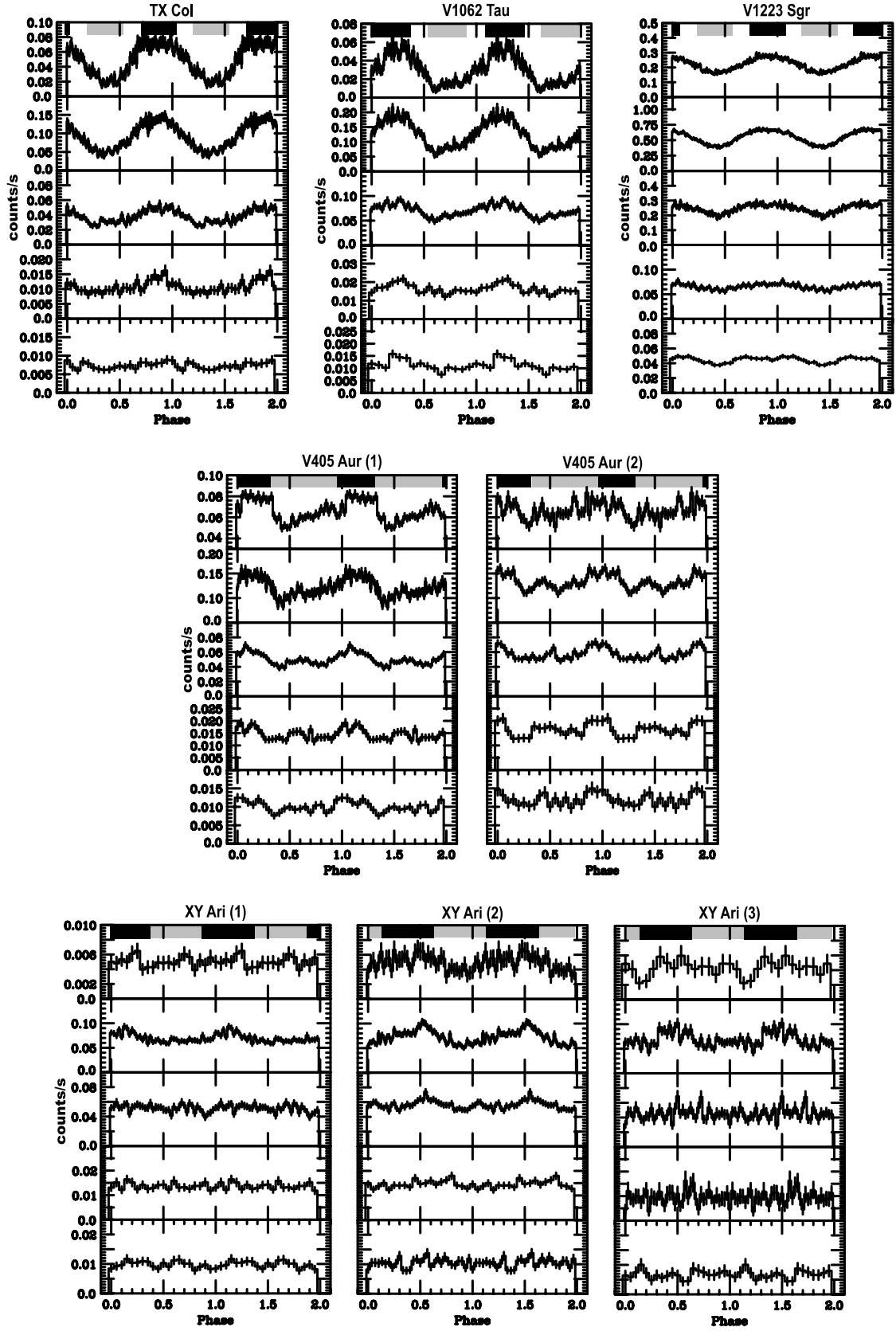
Fig. 2. (Continued.)
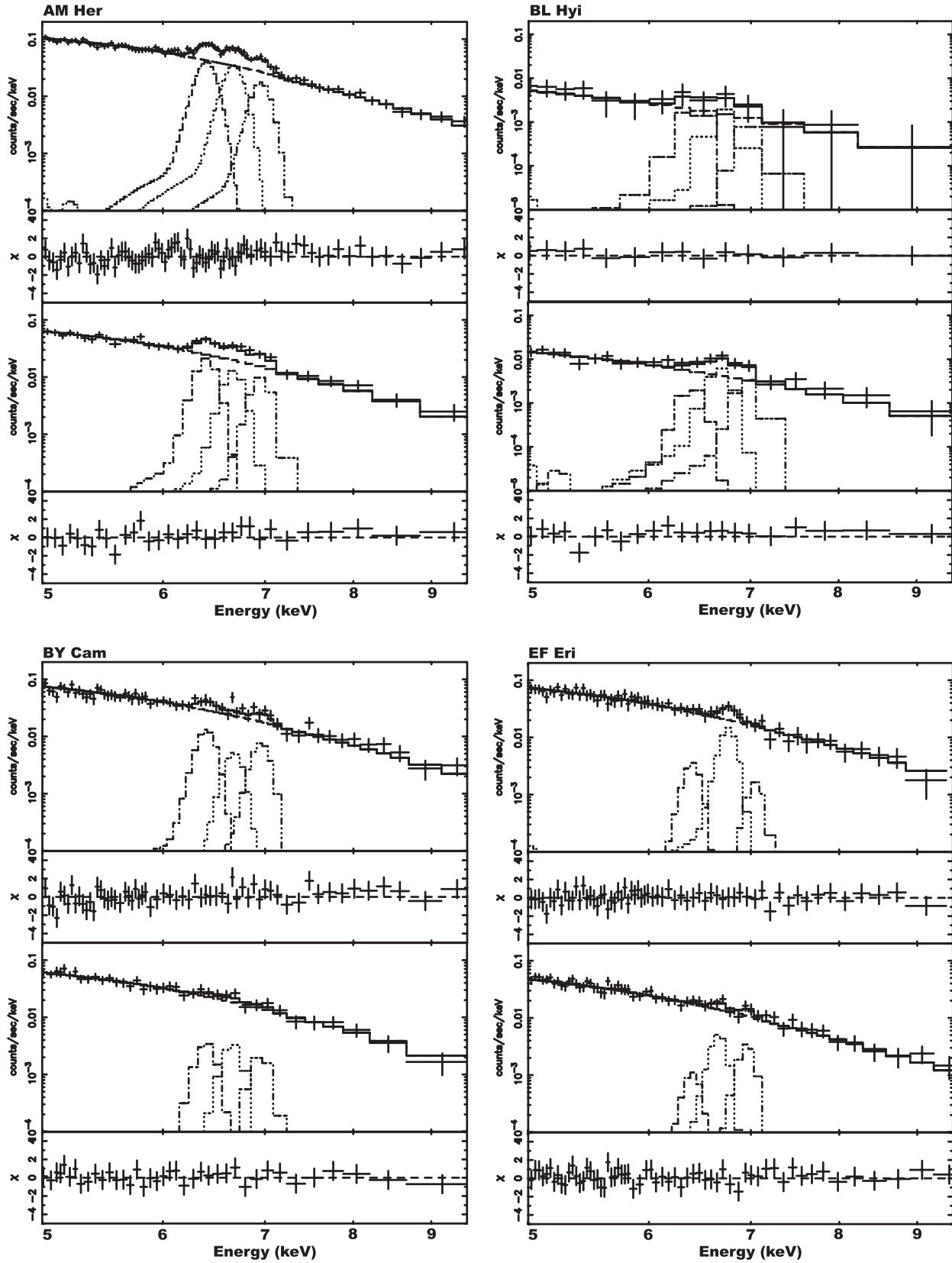
Fig. 3. Phase resolved spectra near the Fe energy band of the polars in our sample, acquired with ASCA. The top panels show the pole-on spectra, and the bottom panels the side-on spectra. Only the SIS data are shown in this figure. The best-fit models, obtained by simultaneous fitting the GIS and SIS data, are also plotted, after convolving with the detector response.
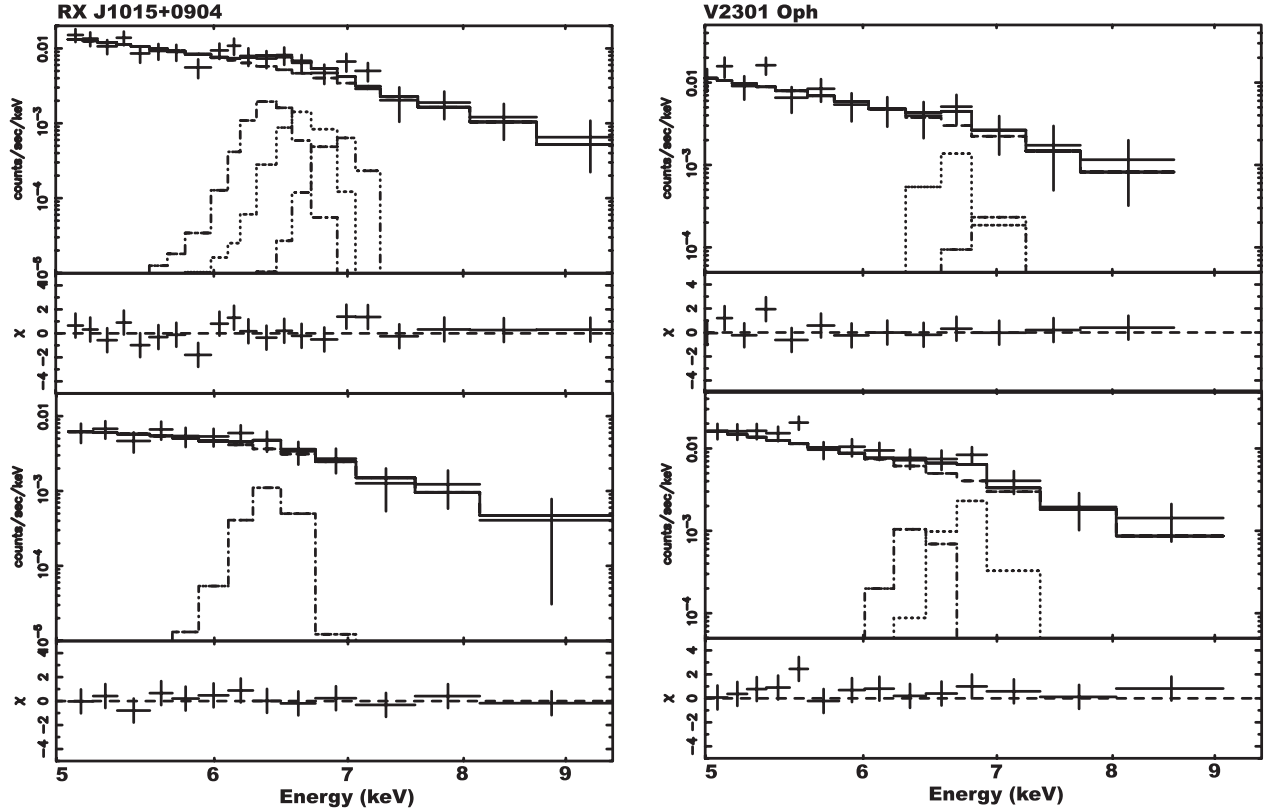
Fig. 3. (Continued.)

occasional errors in the on-board CPU, as well as the SIS data acquired when the field of view was within $10°$ of the bright Earth rim, or when the spacecraft crossed the day-night transition zones.

3. Data Analysis and Results

3.1. X-Ray Light Curves

To perform phase-resolved analysis, we folded X-ray light curves of the selected objects listed in table 1 on their rotational periods. As shown in figure 1, the polars mostly exhibit single-peaked folded light curves in the high-energy band, indicating that we were observing a single pole. The deep X-ray minima seen in some polars to higher energies are due to the self-eclipse of the emission region, while the residual mild X-ray intensity modulations during the uneclipsed phase are explained in terms of the varying contribution from the scattered and/or reflected component from the surface of the WDs (Beardmore et al. 1995). Therefore, the phase of the maximum X-ray intensities roughly corresponds to the pole-on phase ($\theta \sim 0$), or the phase where our line of sights came closest to the accretion-column axis (minimum θ). In addition, in figure 1, the light curves often exhibit absorption dips for softer energies at the X-ray maximum phase. Since these dips arise due to photoelectric absorption by pre-shock matter in the accretion column, they can be used as an additional indicator of the pole-on phase. In this way, we have determined the pole-on and side-on phases of our target sources, as shown by the gray and black bands, respectively, in figure 1. Utilizing the

geometric parameters summarized in table 4 of Paper I, we excluded the phase $\theta > 90°$, in which the emission region is eclipsed by the WD.

For the phase determination of the IPs shown in figure 2, we had to rely solely on the X-ray spin modulations, because of a lack of optical polarization. According to phase-resolved spectroscopy with Ginga (Ishida 1991), the X-ray minimum phase is thought to correspond to the pole-on phase, because the X-ray modulation is due to photoelectric absorption by pre-shock matter (Rosen et al. 1988), as evidenced by the deeper X-ray modulations in the softer energy bands. This idea of self-absorption is supported by Doppler measurements of He II emission lines from the pre-shock matter (Hellier et al. 1987, 1990). We have thus defined the pole-on and side-on phases, as shown by the gray and black bands, respectively, in figure 2.

3.2. Phase-Resolved Spectra

We accumulated ASCA spectra separately over the pole-on and side-on phases, as shown in figures 3 and 4 for the polars and IPs, respectively. To quantify the EWs of the Fe lines, we adopted the standard spectral model, i.e., a photoelectrically absorbed bremsstrahlung continuum with three narrow Gaussians (Ezuka, Ishida 1999; Paper I), the latter representing neutral (at 6.4 keV), He-like (at ~ 6.7 keV), and H-like (at ~ 6.9 keV) Fe Kα lines. The three lines can be resolved with the SIS, but not with the GIS. Accordingly, we fixed the centroid energies of the first Gaussian at 6.4 keV, fixed the ratio of the centroid energies of the others at the theoretical value of 1.042, and assumed them to be narrow. The energy range for
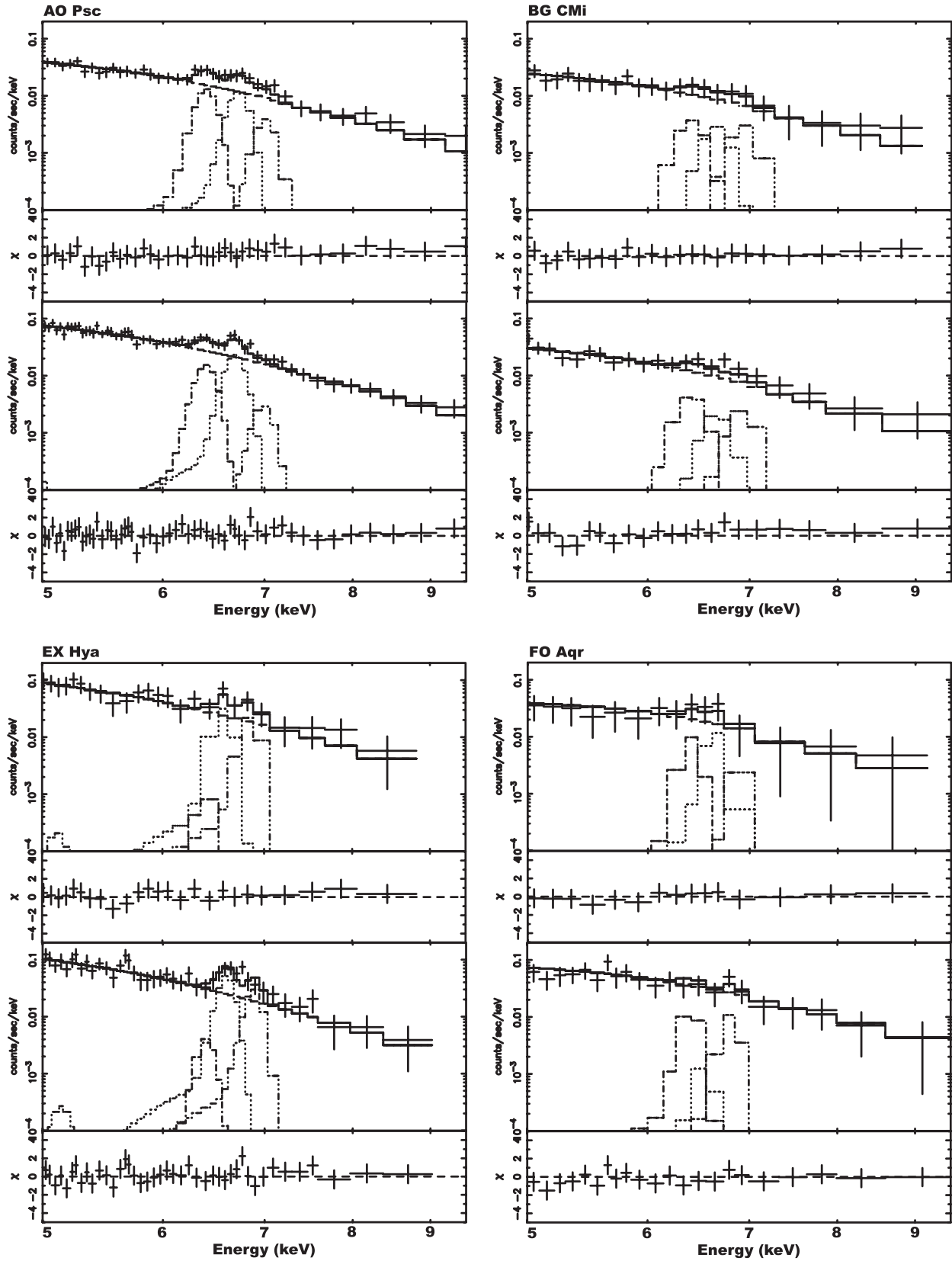
Fig. 4.   Similar to figure 3, but for the IPs in our sample.

Fig. 4. (Continued.)

V1062 Tau

V1223 Sgr

V405 Aur

XY Ari
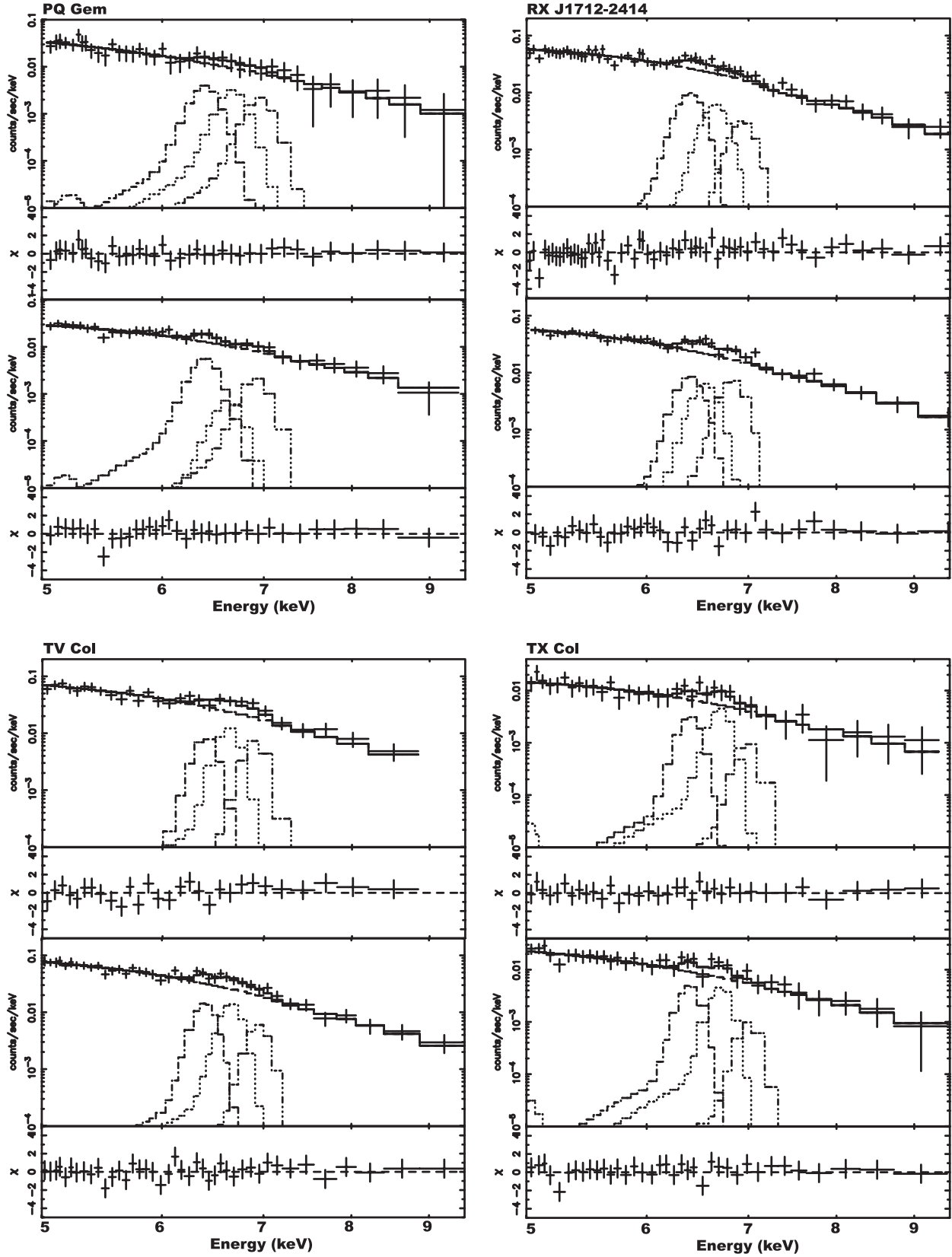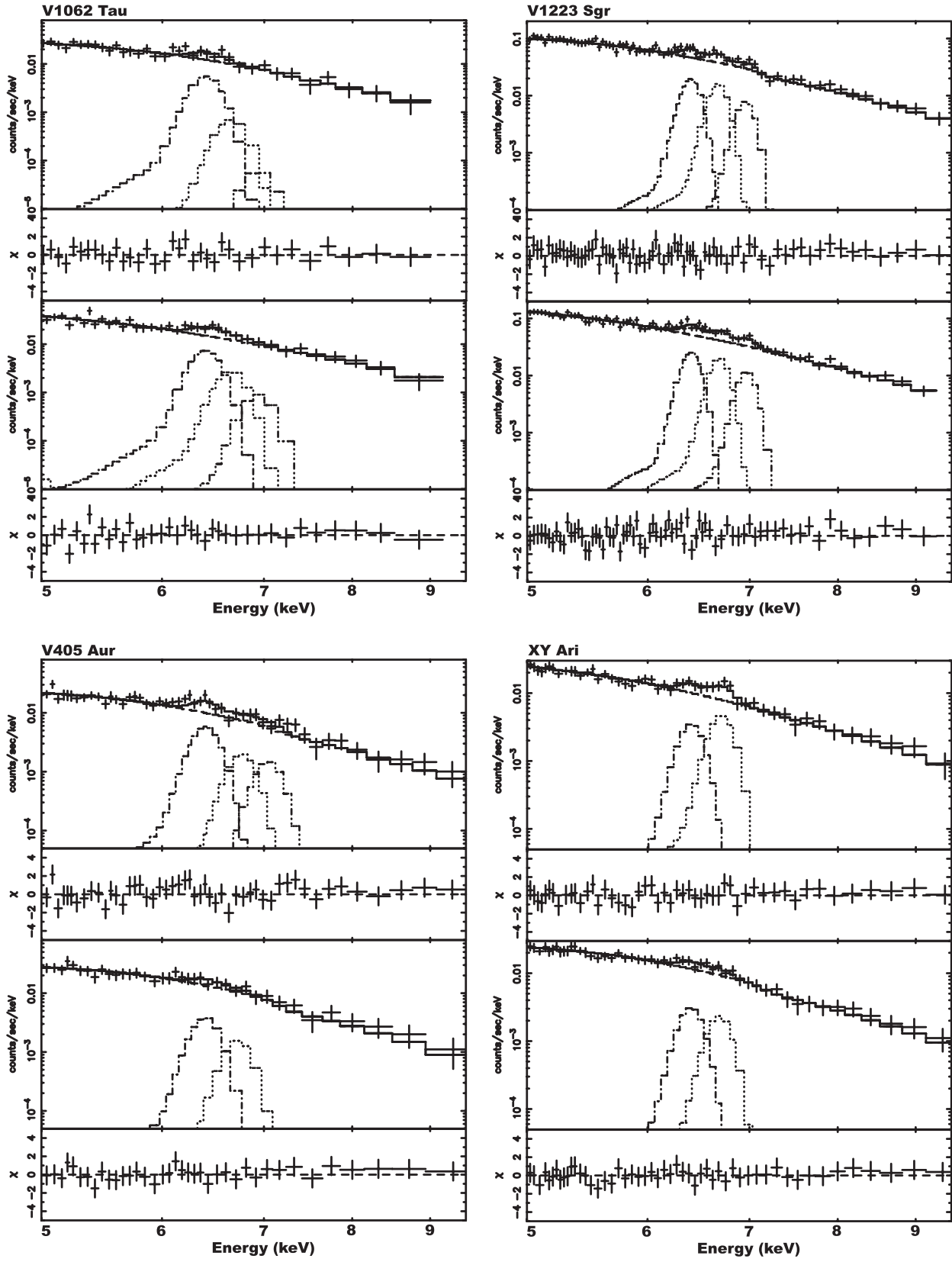
Fig. 4. (Continued.)
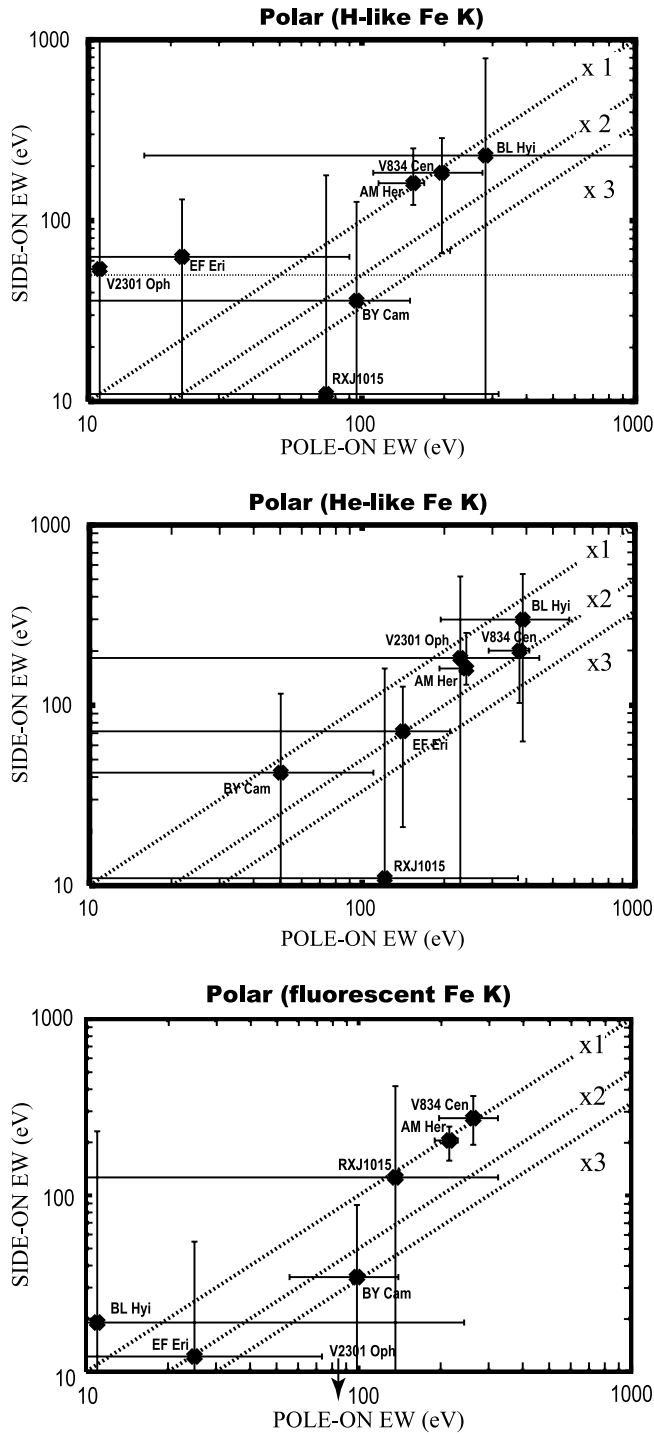
Fig. 5. Fe line EWs of the polars measured at the pole-on phase, compared with those at the side-on phase. The top and middle panels are for H-like and He-like Fe K lines, respectively. For a reference, the EWs of fluorescent Fe K lines are plotted in the bottom panel.

Fig. 6. Same as figure 5, but for the IPs.

the continuum fitting was optimized in the manner described in section 3.2 of Ezuka and Ishida (1999). The SIS and GIS spectra were fitted simultaneously. The fits were successful, as shown in figures 3 and 4, where we compare predictions of the best-fit model with the actual data.

Figure 5 compares the EWs of the H-like and He-like Fe Kα lines of individual polars for their pole-on and side-on phases. Figure 6 presents the same comparison for the IPs. For a reference, the EWs of the fluorescent Fe Kα line, which is not emitted from the hot accretion columns, but probably from the WD surfaces, are also plotted in the same figures. As is clearly demonstrated by figure 5, the EWs of the He-like Fe line of our sample polars are systematically larger in the
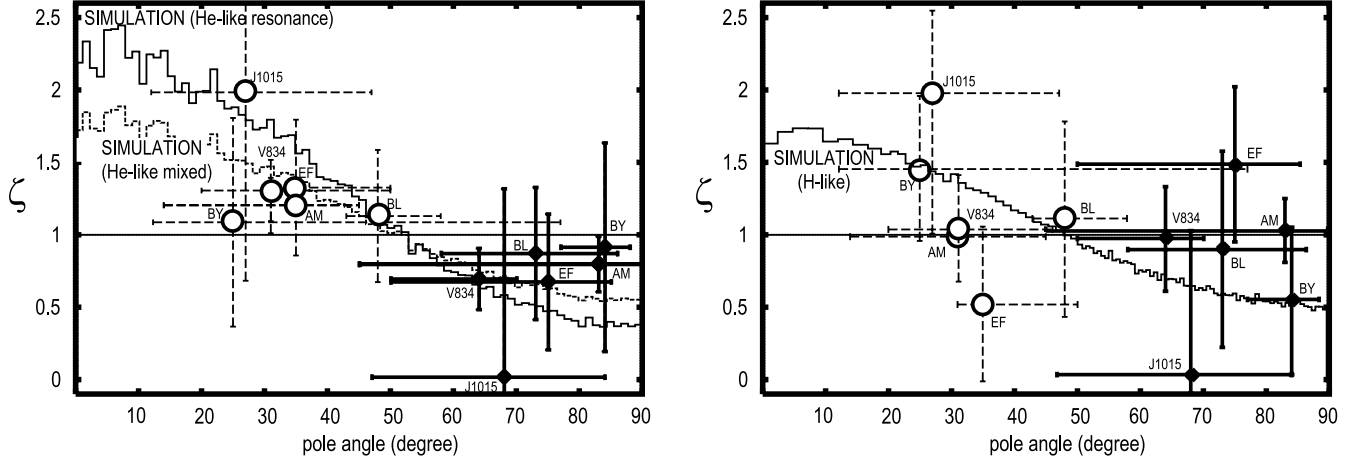
Fig. 7. EWs of He-like (left) and H-like (right) Fe lines of the 7 polars in their pole-on and side-on phases, relative to the phase-averaged value. The data of V2301 Oph are not plotted, because the geometrical parameters are not available. They are presented against the pole angle, θ, which was calculated using the geometrical parameters in table 4 of Paper I. Each object appears twice, with the circle for the pole-on data and with the filled diamond for the side-on data. The angular distributions predicted by the Monte Carlo simulation (Paper I) in the nominal case are also plotted, assuming a temperature of 16 keV, a bulk velocity of the plasma of $0.9 \times 10^8 \, \mathrm{cm \, s^{-1}}$, an electron density of $7.7 \times 10^{15} \, \mathrm{cm^{-3}}$ just below the shock front, and a column radius of 7.0×10^7 cm.

pole-on phase than in the side-on phase, although the enhancement in individual objects is insignificant, and that of the H-like line is consistent with being unmodulated. Quantitatively, the enhancements of the H-like and He-like Fe K lines, weighted by the absolute values of their EWs, are $\zeta_{\mathrm{OBS}}^{\mathrm{P}}(\mathrm{H}) = 1.05 \pm 0.47$ and $\zeta_{\mathrm{OBS}}^{\mathrm{P}}(\mathrm{He}) = 1.88 \pm 0.72$, respectively (90% confidence errors). The value is slightly changed to $\zeta_{\mathrm{OBS}}^{\mathrm{P}}(\mathrm{H}) = 1.05 \pm 0.53$ and $\zeta_{\mathrm{OBS}}^{\mathrm{P}}(\mathrm{He}) = 1.89 \pm 0.86$, when we exclude the data of V834 Centauri, which were already presented in Paper I. Our result for the sample of polars therefore confirms the enhancement of the He-like line in a statistical sense. For the IPs, we see no modulation in either Fe line (figure 6); the enhancements of the H-like and He-like Fe K lines are $\zeta_{\mathrm{OBS}}^{\mathrm{IP}}(\mathrm{H}) = 1.02 \pm 0.47$ and $\zeta_{\mathrm{OBS}}^{\mathrm{IP}}(\mathrm{He}) = 1.14 \pm 0.36$, respectively.

4. Discussion

In order to confirm the general validity of the anisotropic transfer scenario of resonance photons in MCVs pointed out in Paper I, we systematically analyzed the ASCA data of 7 polars and 12 IPs. Through a phase-resolved analysis of the ionized Fe $K\alpha$ lines, the EWs of the He-like Fe lines of the polars were found to be systematically enhanced in their pole-on phases. Although the significance is only 90%, and the individual cases were insignificant, except for V834 Centauri (Paper I), the statistical trend is in support of our scenario. To better visualize this result, in figure 7, left panel, the EWs of the He-like Fe lines of the polars are plotted relative to the phase-averaged value, as a function of θ. There, the results of our Monte Carlo simulations are also plotted based on representative parameters (see caption). Thus, the observed spin-phase dependence of the Fe-K line EWs is consistent with the calculation, although within rather large errors.

The observed He-like Fe line is, in fact, a blend of resonance, forbidden, and intercombination lines, where the latter two do not suffer the resonance effect. Since the H-like line is a
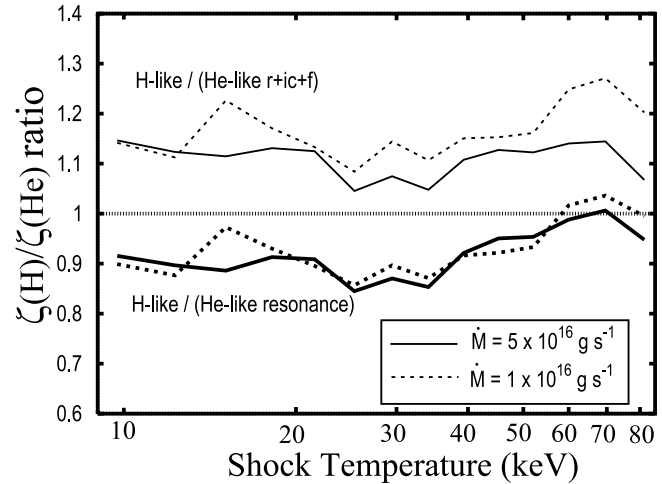
Fig. 8. Comparison of the anisotropic effects for the H-like and He-like Fe $K\alpha$ lines, based on our Monte Carlo simulation. The ratio of the enhancement, ζ, at the exact pole-on direction ($\theta = 0$) of H-like and He-like Fe $K\alpha$ lines is shown as a function of the mass-accretion rate, $5 \times 10^{16} \, \mathrm{g \, s^{-1}}$ and $1 \times 10^{16} \, \mathrm{g \, s^{-1}}$. Calculations were made for the same sets of conditions as in Paper I (shown in the caption to figure 7).

pure resonance line, we may expect to observe a larger spin modulation for this line compared to that of the He-like blend. According to our Monte Carlo simulations (Paper I; Terada 2002), however, the expected enhancement of the H-like Fe line is actually smaller than that of the He-like resonance line, because the former photons are preferentially produced in a higher portion of the post-shock column, which has lower densities and smaller velocity differences than those at the bottom of the column (Aizu 1973). As presented in figure 8, we expect almost the same enhancement of the H-like Fe line as that of the He-like blend. Furthermore, the H-like Fe K

line is subject to rather large measurement errors, due to its relatively poor statistics and its possible confusion with the Fe Kβ emission line from He-like iron. As a result, the measurements of the H-like Fe line EWs (figures 5, 6, and 7 right) are consistent with the prediction.

As for IPs (figure 6), the modulations of both line species have been found to be statistically insignificant. One possible explanation is that the accretion streams of IPs have a curtain-like shape (Rosen et al. 1988), with a much-reduced optical depth in the lateral direction, so that the anisotropic resonance effect is suppressed. Alternatively, the emission region may have a column shape, like polars, and the lack of spin modulation in the Fe line EWs may be attributed to higher electron densities, n_e, in the plasma, as is indicated by their larger volume emission measure (VEM, described as $\int n_e^2 dV$, where V is the plasma volume) than those of polars. Then, the enhanced Compton scattering by hot electrons reduces the anisotropic effect on the resonance photons (see figure 8 in Paper I). In fact, by comparing figure 5 with figure 6, we find that the IPs exhibit systematically smaller EWs of Fe Kα lines than the polars.

In order to examine the latter possibility for the IPs, figure 9 shows plots of VEMs of the polars and IPs listed in table 1, which shows that the VEMs of IPs are one-to-two orders of magnitude larger than those of polars. Then, adopting the same discussion as in subsection 5.2 of Paper I, we estimate that the accretion column of an IP has an order-of-magnitude higher electron density of $n_e \sim 10^{17}\,\mathrm{cm}^{-3}$, an order-of-magnitude lower column height of $h \sim 10^6\,\mathrm{cm}$, and a several-times larger column radius of $r \sim 10^7\,\mathrm{cm}$, all compared with polars. Under such conditions, the optical depth to Compton scattering is ~ 1.0, whereas it is only 0.4 for polars. Therefore, the interpretation may actually work.

The Fe-K line photons provide the best diagnostics of the resonance effects, because Fe ions are massive enough for the thermal Doppler effect to fall significantly below the bulk-motion Doppler shift. Although the ASCA data of MCVs are rather limited both in statistics for phase-resolved analyses and
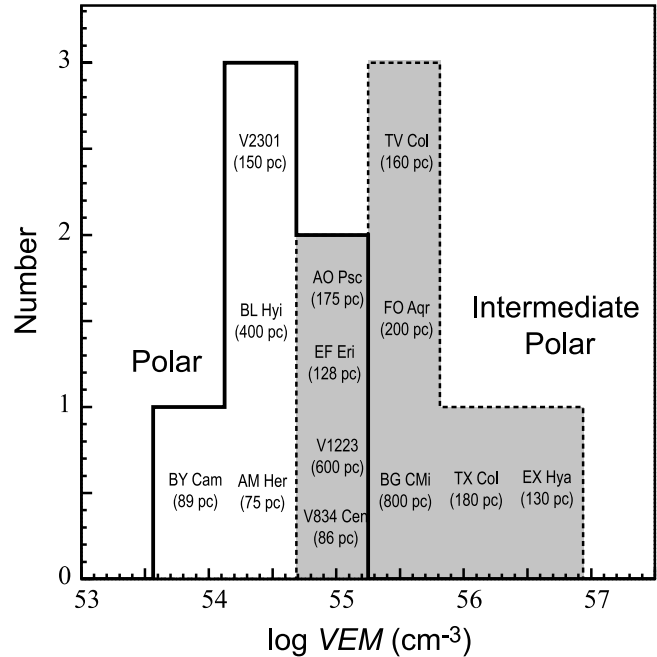
Fig. 9. Distribution of the measured emission measure of polars (thick solid histogram) and IPs (dashed lines with shadows) given in table 1. The object names and their distances are also shown in this figure.

energy resolution, a quantum jump in this research subject may be realized by the Astro-E2 satellite to be launched in 2005, with its energy resolution reaching $\sim 10\,\mathrm{eV}$ around the Fe Kα line range for the first time.

References

Aizu, K. 1973, Prog. Theor. Phys., 49, 1184
Augusteijn, T., Heemskerk, M. H. M., Zwarthoed, G. A. A., & van Paradijs, J. 1994, A&AS, 107, 219
Barwig, H., Ritter, H., & Barnbantner, O. 1994, A&A, 288, 204
Beardmore, A. P., Done, C., Osborne, J. P., & Ishida, M. 1995, MNRAS, 272, 749
Bond, I. A., & Freeth, R. V. 1988, MNRAS, 232, 753
Buckley, D. A. H., Haberl, F., Motch, C., Pollard, K., Schwarzenberg-Czerny, A., & Sekiguchi, K. 1997, MNRAS, 287, 117
Burke, B. E., Mountain, R. W., Harrison, D. C., Bautz, M. W., Doty, J. P., Ricker, G. R., & Daniels, P. J. 1991, IEEE Trans. Nucl. Sci., ED-38, 1069
Cropper, M. 1985 MNRAS, 212, 709
Ezuka, H., & Ishida, M. 1999, ApJS, 120, 277
Fujimoto, R., & Ishida, M. 1997, ApJ, 474, 774
Heise, J., & Verbunt, F. 1988, A&A, 189, 112
Hellier, C. 1997, MNRAS, 288, 817
Hellier, C., Mason, K. O., & Cropper, M. 1990, MNRAS, 242, 250
Hellier, C., Mason, K. O., Rosen, S. R., & Córdova, F. A. 1987, MNRAS, 228, 463
Hoshi, R. 1973, Prog. Theor. Phys., 49, 776
Ishida, M. 1991, PhD Thesis, The University of Tokyo
Ishida, M., Greiner, J., Remillard, R. A., & Motch, C. 1998, A&A, 336, 200
Kaluzny, J., & Semeniuk, I. 1988, Inf. Bull. Variable Stars, 3145
Makishima, K., et al. 1996, PASJ, 48, 171
Mennickent, R. E., Diaz, M. P., & Arenas, J. 1999, A&A, 352, 167
Mewe, R., Gronenschild, E. H. B. M., & van den Oord, G. H. J. 1985, A&AS, 62, 197
Misaki, K., Terashima, Y., Kamata, Y., Ishida, M., Kunieda, H., & Tawara, Y. 1996, ApJ, 470, L53
Norton, A. J., Hellier, C., Beardmore, A. P., Wheatley, P. J., Osborne, J. P., & Taylor, P. 1997, MNRAS, 289, 362
Ohashi, T., et al. 1996, PASJ, 48, 157
Patterson, J. P. 1994, PASP, 106, 209
Piirola, V., Coyne, G. V., Takalo, S. J., Takalo, L., Larsson, S., & Vilhu, O. 1994, A&A, 283, 163

Rosen, S. R., Mason, K. O., & Córdova, F. A. 1988, MNRAS, 231, 549

Schwope, A. D., Thomas, H.-C., Beuermann, K., & Reinsch, K. 1993, A&A, 267, 103

Shafter, A. W., & Macry, J. D. 1987, MNRAS, 228, 193

Skillman, D. R. 1996, PASP, 108, 130

Takano, S., et al. 1989, IAU Circ., 4745, 1

Tanaka, Y., Inoue, H., & Holt, S. S. 1994, PASJ, 46, L37

Terada, Y. 2002, PhD Thesis, The University of Tokyo

Terada, Y., Ishida, M., Makishima, K., Imanari, T., Fujimoto, R., Matsuzaki, K., & Kaneda, H. 2001, MNRAS, 328, 112 (Paper I)

Terada, Y., Kaneda, H., Makishima, K., Ishida, M., Matsuzaki, K., Nagase, F., & Kotani, T. 1999, PASJ, 51, 39